Investigation of homogeneous photosensitized oxidation activities of palladium and platinum octasubstituted phthalocyanines: Oxidation of 4-nitrophenol

Taofeek B. Ogunbayo, Edith Antunes, Tebello Nyokong *

Department of Chemistry, Rhodes University, Grahamstown 6140, South Africa
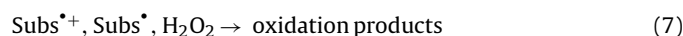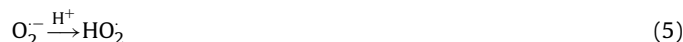
ABSTRACT

Photosensitized oxidation of 4-nitrophenol was studied in organic solutions with seven octasubstituted thio and aryloxy palladium and platinum phthalocyanines acting as photosensitizers. Kinetic studies conducted also showed that the complexes have different singlet oxygen quenching constants with direct implication on the quantum yield of photodegradation of 4-nitrophenol ($\Phi_{4\text{-NP}}$). Palladium analogues gave better results than the platinum analogues in terms of $\Phi_{4\text{-NP}}$ with palladium-(dodecylthio)phthalocyanine giving the highest yield of 1.8×10^{-3}. Gas chromatography (GC) and liquid chromatography connected to a mass spectrometer (LC–MS) were used to confirm the photodegradation products which were hydroquinone and 1,4-benzoquinone.
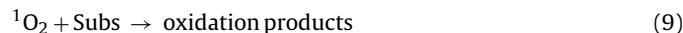
© 2010 Elsevier B.V. All rights reserved.

1. Introduction

Photodegradation of pollutants is gaining extensive attention in the quest for efficient and benign conversion processes in the area of environmental management. Photosensitized catalysis is the initiation of degradation or transformation reactions of molecules using a combination of light and photoactive materials as catalysts.

Photosensitization of a reaction may proceed through two reaction pathways namely Type I and Type II mechanisms [1–4]. Type I mechanism (Eqs. (1)–(7)) involves the transformation of the photogenerated triplet state (Eq. (1)) of a photosensitizer such as a metallophthalocyanine (^{3}MPc*) into a radical specie (MPc$^{\bullet+}$) via electron transfer interaction with ground state molecular oxygen (^{3}O$_2$), Eq. (2). The excited triplet state of the MPc (^{3}MPc*) can also interact with ground state molecular oxygen (Eq. (4)) generating superoxide and other radicals (including OH$^\bullet$, O$_2^{\bullet-}$ HO$_2^\bullet$) which subsequently afford oxidation of the substrate (Eqs. (5)–(7)) by a Type I mechanism. The excited triplet state of the MPc (^{3}MPc*) can also interact with the substrate molecules, Eq. (3) to give radical species.

$$\text{MPc} \rightarrow {}^1\text{MPc}* \rightarrow {}^3\text{MPc}* \tag{1}$$

$$^3\text{MPc}^* + \text{O}_2 \rightarrow \text{MPc}^{\bullet+} + \text{O}_2^{\bullet-} \tag{2}$$

$$^3\text{MPc}^* + \text{Subs} \rightarrow \text{MPc}^{\bullet-} + \text{Subs}^{\bullet+} \tag{3}$$

$$\text{MPc}^{\bullet-} + \text{O}_2 \rightarrow \text{MPc} + \text{O}_2^{\bullet-} \tag{4}$$

$$\text{O}_2^- \xrightarrow{\text{H}^+} \text{HO}_2^\cdot \tag{5}$$

$$\text{HO}_2^\bullet + \text{Subs-H} \rightarrow \text{H}_2\text{O}_2 + \text{Subs}^\bullet \tag{6}$$

$$\text{Subs}^{\bullet+}, \text{Subs}^\bullet, \text{H}_2\text{O}_2 \rightarrow \text{oxidation products} \tag{7}$$

The Type II (Eqs. (8) and (9)) mechanism starts with the energy transfer interaction between triplet state of the photosensitizers (^{3}MPc*) and ground state molecular oxygen (^{3}O$_2$) to give energetic singlet oxygen (^{1}O$_2$), Eq. (8), which is capable of oxidizing the substrate, Eq. (9).

$$^3\text{MPc} * + {}^3\text{O}_2 \rightarrow {}^1\text{O}_2 \tag{8}$$

$$^1\text{O}_2 + \text{Subs} \rightarrow \text{oxidation products} \tag{9}$$

Metallophthalocyanines (MPcs) with their high absorption in the visible region and non-destructive singlet to energetic triplet state transition have been shown to photosensitize reactions mainly through Type II mechanism. Considerable singlet to triplet state transition and long life time of the triplet state are major factors influencing successful singlet oxygen generation by MPc complexes. MPc complexes containing large central metals are the best choice for photosensitized reactions due to enhanced intersystem crossing while closed shell diamagnetic metals improve triplet state lifetime as against open-shell metals [5–9].

Photosensitized oxidation of phenols using MPc complexes has been reported under both heterogeneous and homogeneous conditions [10–17]. Even though heterogeneous conditions are preferred in terms of ease of regeneration of the catalyst, homogeneous reaction leads to a better understanding of mechanisms involved
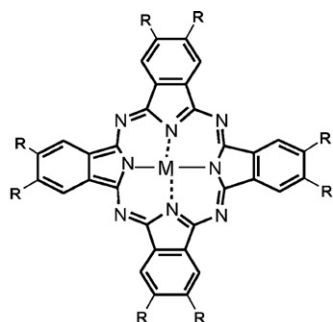
1a; R = S-C$_5$H$_{11}$

1b; R = S-C$_8$H$_{17}$

1c; R = S-C$_{12}$H$_{25}$

M = Pd (1)

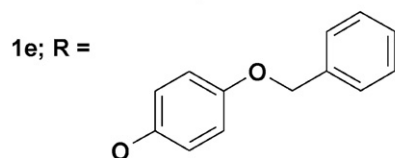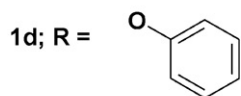**M = Pt (2)**

1d; R =

1e; R =

Fig. 1. Structures of the PtPc and PdPc complexes employed as photosensitizers in this work.

and improvement of the catalytic activity. The MPc photosensitized oxidation of 4-nitrophenol (4-NP) has been reported under homogeneous conditions [10], and the products obtained were 4-nitrocatechol and hydroquinone. However considerable degradation of the MPc photosensitizers was observed in some cases. The search for photoresistant catalysts that can degrade 4-nitrophenol to products of reduced toxicity led to the use, in this work, of phthalocyanine complexes containing open-shell diamagnetic central metals: PtPc and PdPc.

In spite of their open-shell nature which theoretically is a shortcoming due to short triplet lifetimes, PdPc and PtPc complexes show high singlet oxygen quantum yields suggesting that their lower lifetimes are still high enough for efficient application as photosensitizers [18]. In addition, PdPcs have been found to show higher photostability compared to other metallo phthalocyanines [19,20]. PdPcs and PtPcs photosensitized oxidation of 4-nitrophenol is reported in this work for the first time.

2. Experimental

2.1. Materials

Dichloromethane (DCM), 4-nitrophenol, fumaric acid, 4-nitrocatechol and hydroquinone were purchased from SAARCHEM. Diphenylisobenzofuran (DPBF) was purchased from Aldrich. The syntheses of the photosensitizers (phthalocyanine complexes, Fig. 1): 2,3,9,10,16,17,23,24-octakis(pentylthiophthalocyaninato) palladium(II) (**1a**), 2,3,9,10,16,17,23,24-octakis(octylthiophthalocyaninato) palladium(II) (**1b**), 2,3,9,10,16,17,23,24-octakis(dodecylthiophthalocyaninato)palladium(II) (**1c**), palladium-2,3,9,10,16,17,23,24-octakis(phenoxy)phthalocyanine (**1d**), 2,3,9,10,16,17,23,24-octakis(benzyloxyphenoxy)phthalocyaninato palladium (**1e**), 2,3,9,10,16,17,23,24-
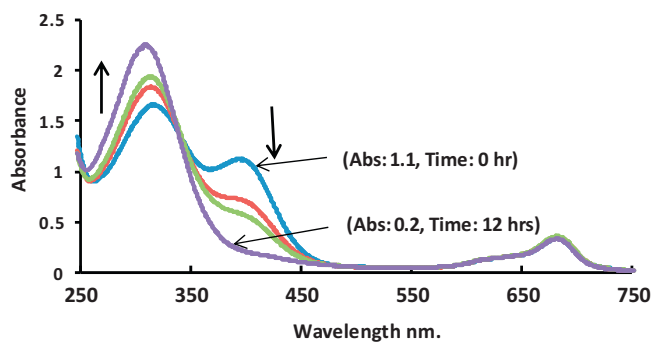
octakis(phenoxy)phthalocyaninato platinum (**2d**) and 2,3,9,10,16,17,23,24-octakis(benzyloxyphenoxy)phthalocyanato platinum (**2e**) have been reported before [18].

2.2. Equipment and photosensitized oxidation procedures

The irradiation experiments were carried out using a tungsten lamp (100 W, 30 V) perpendicular to the direction of measurement. A 600 nm glass cut off filter (Schott) and a water filter were used to filter off ultraviolet and infrared radiation respectively. An interference filter (Intor, 670 nm with a band width of 40 nm) was additionally placed in the light path before the sample, to ensure the excitation of the Q band.

The intensity of the light reaching the reaction vessel was measured with a power meter (POWER MAX 5100, Molelectron Detector Inc.) and was found to be 3.5×10^{20} photons cm^{-2} s^{-1}. The transformation of the analyte was monitored through the absorption peak at 400 nm after each photolysis cycle using a Shimadzu UV-2550 UV–vis spectrophotometer. A 1 cm pathlength UV–vis spectrophotometric cell, fitted with a tight fitting stopper was used as the reaction vessel. Experiments were carried out in DCM in

Fig. 2. Electronic absorption spectral changes observed during the photolysis of 6.5×10^{-4} mol L^{-1} 4-NP in the presence of 350 mg L^{-1} of complex **1c** in DCM.
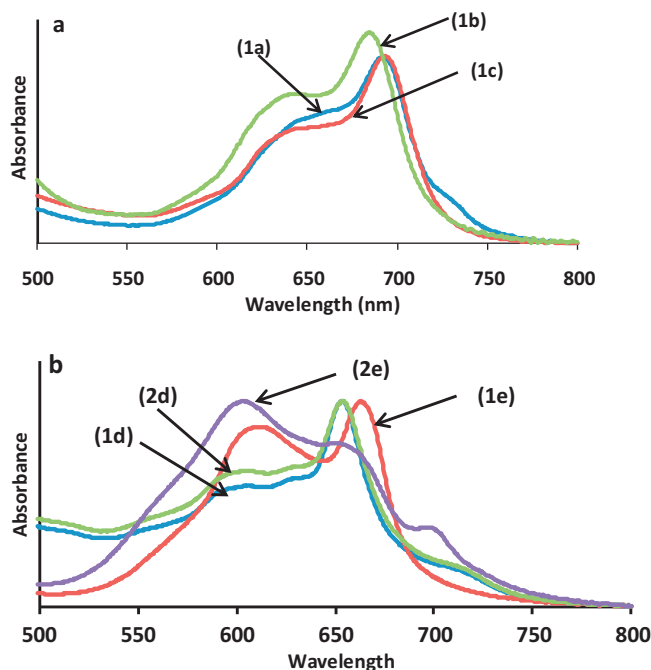

Fig. 3. Spectra of (a) alkylthio derivatised phthalocyaines **1a**, **1b** and **1c** and (b) aryloxy derivatised phthalocyanines **1d**, **1e**, **2d** and **2e**. Concentration ~1 × 10^{-5} mol L^{-1} in DCM.

Table 1
Complexes' photosensitization parameters for phototransformation of 4-NP (3.5×10^{-4} M, DCM).

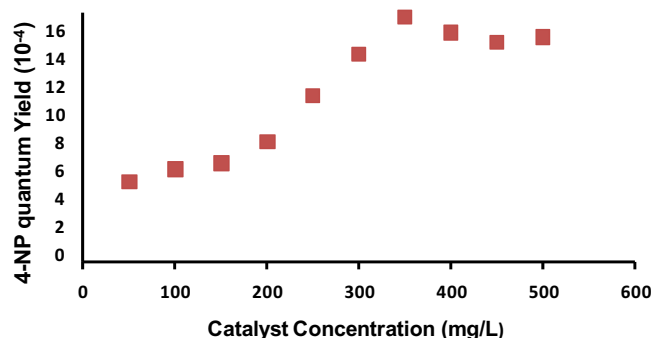| Complexes	Optimum photosensitizer concentration (mg L^{-1})	$\Phi_{4\text{-NP}}$ (10^{-4})	Φ_{Δ} (DCM)	$k_r = k_d/\Phi_{\Delta}$ slope (mol^{-1} L s^{-1})	$k_q + k_r$ (mol^{-1} L s^{-1})
(**1a**)	200	14	0.38	1.80×10^5	1.6×10^9
(**1b**)	300	15	0.36	1.70×10^5	2.7×10^8
(**1c**)	350	18	0.39	2.00×10^5	3.0×10^8
(**1d**)	250	9	0.30	1.40×10^5	3.1×10^8
(**1e**)	350	16	0.32	1.95×10^5	3.2×10^7
(**2d**)	200	0.3	0.29	2.30×10^5	4.0×10^8
(**2e**)	350	0.7	0.26	2.12×10^5	4.3×10^8

Fig. 4. Plot of $\Phi_{4\text{-NP}}$ vs concentration of photosensitizers to determine the optimum concentration of complex **1c** for the phototransformation of 4-NP (3.5×10^{-4} mol L^{-1}) in DCM.

which both the MPc derivatives and 4-NP were dissolved. Triethylamine was employed to ensure the basicity of the DCM solution since in highly basic media, ensuring that 4-NP is deprotonated.

The products were separated and analysed using both gas chromatography (GC) and high performance liquid chromatography (HPLC) equipment connected in tandem to a mass spectrometer (LC/MS). For the gas chromatography (GC) analysis, an Agilent Technologies 6820 GC system (HP 5973, using an HP-1 this was actually a DB-5MS column) was employed. A dual wavelength UV detector was used for HPLC analyses and the wavelengths used were 254 nm and 318 nm. The HPLC conditions utilized included an Agilent Eclipse XDB-C18 column (150×4.6 (i.d.) mm) 5 μm particle size and a mobile phase with gradient elution starting at 10% MeOH:H$_2$O (pH 5.5 with formic acid) for 10 min and then ramping to 100% MeOH in 10 min. A Finnigan MAT LCQ ion trap mass spectrometer equipped with an electrospray ionization (ESI) source was used for mass analysis. Spectra were acquired in the negative ion mode, with the capillary temperature set at 200 °C and sheath gas set at 80 arbitrary units, with the capillary and tube lens voltages set at −20 and −5 V respectively.
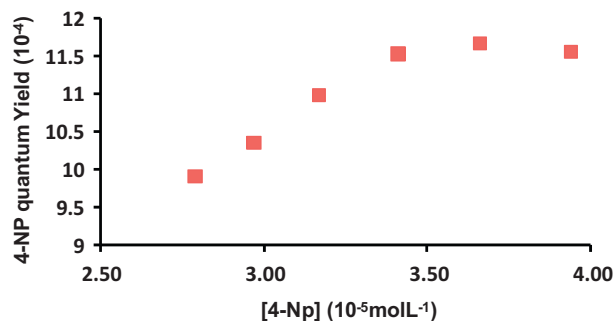
2.3. Singlet oxygen quantum yields

The singlet oxygen quantum yield (Φ_{Δ}) determinations were carried out using solutions containing DPBF (90 μM) as the singlet oxygen quencher and the MPcs (absorbance ~0.2 at the irradiation wavelength). A solution of the MPc complex (2 mL) contained in a quartz 10 mm spectrophotometric cell was saturated with oxygen and irradiated using the set-up described above. The irradiation and measurement were repeated until around 80% decay of DPBF was observed [21]. The DPBF absorbance was corrected for the absorbance of sensitizer at the respective detection wavelength.

Fig. 5. Plot of $\Phi_{4\text{-NP}}$ vs concentration of 4-NP for phototransformation of 4-NP in the presence of complex **1b** (300 mg L^{-1}) in DCM.
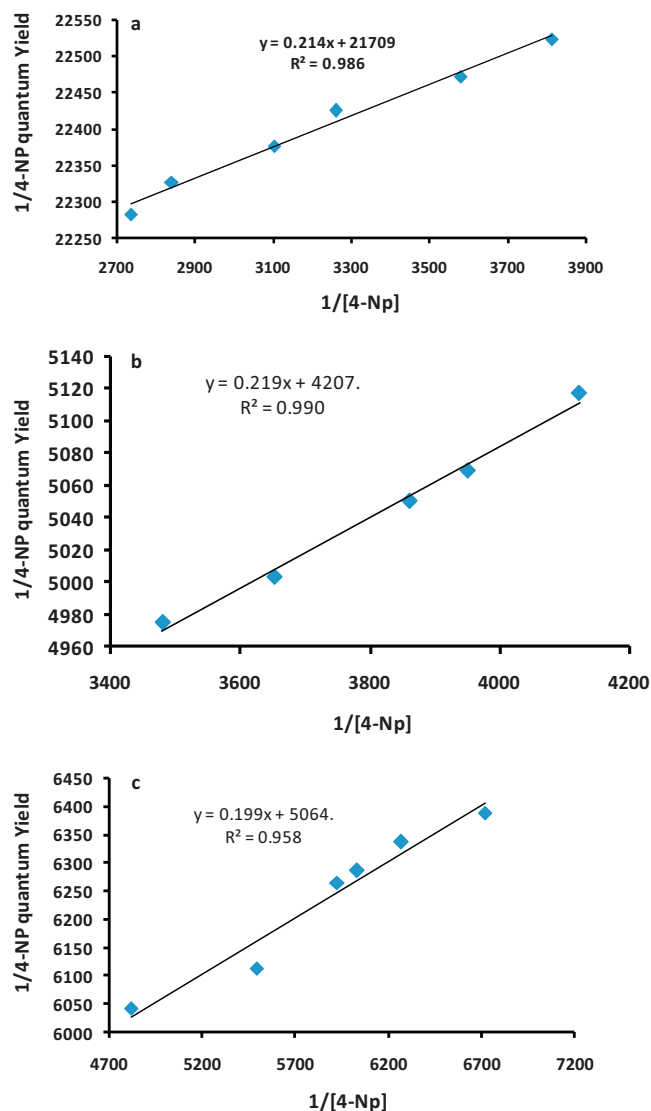
Fig. 6. Plots of $1/\Phi_{4\text{-NP}}$ vs $1/[4\text{-NP}]$ in the photo-oxidation of 4-nitrophenol for complexes (a) **1a** (200 mg L^{-1}), (b) **1c** (350 mg L^{-1}) and (c) **1e** (350 mg L^{-1}) in DCM.
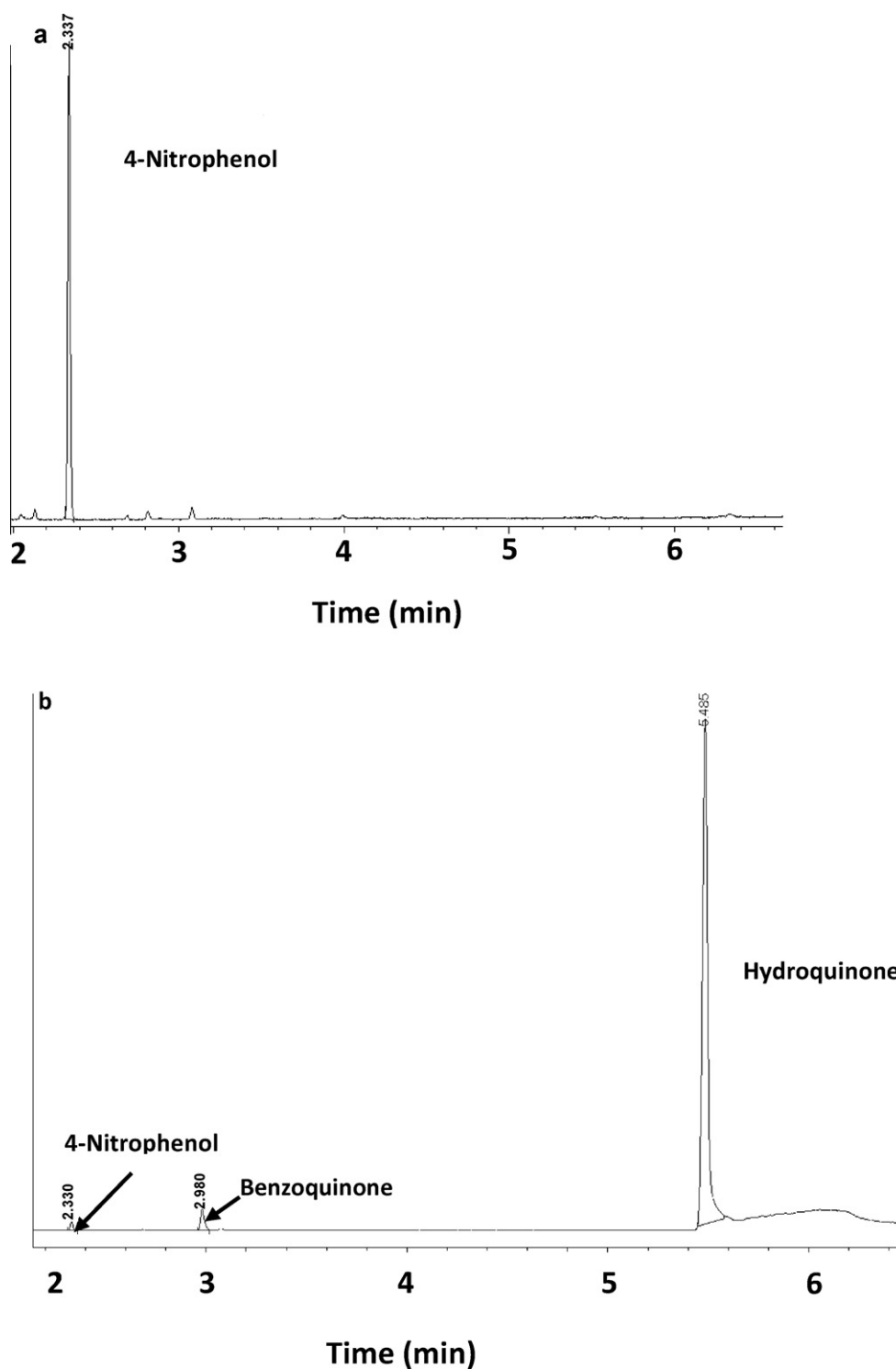
Fig. 7. Gas chromatogram for heterogeneous photosensitized oxidation of 4-nitrophenol by complex **1c** (a) before irradiation and (b) after irradiation for 12 h. Concentrations of **1c** = 350 mg L^{-1} and 4-nitrophenol = 3.5 × 10^{-4} mol L^{-1} in DCM.

The DPBF quantum yield Φ_{DPBF} was calculated using Eq. (10)

$$\Phi_{DPBF} = \frac{[C_o - C_t]V}{I_{abs}t} \tag{10}$$

where C_o and C_t are the concentrations of DPBF before and after irradiation respectively, V is the volume of the sample in the cell; t

is the irradiation time. I_{abs} is given by Eq. (11)

$$I_{abs} = \frac{\alpha AI}{N_A} \tag{11}$$

where α is the fraction of light absorbed, A is the cell area irradiated, I is the light intensity from the lamp and N_A is the Avogadro's constant. The determined extinction coefficient of DPBF in DCM (ε_{CNP} = 21,100 L^{-1} mol cm^{-1}) was employed.
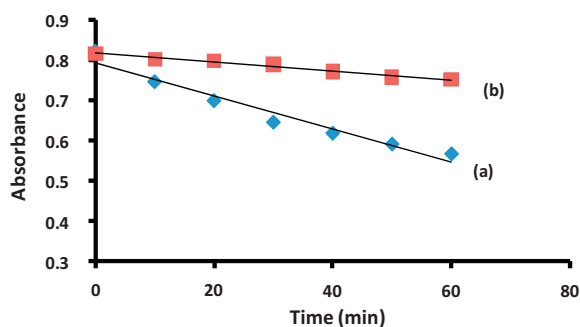
Fig. 8. Absorption spectral changes observed for photosensitized transformation of 4-NP in the absence (a) and presence and (b) of sodium azide. Concentrations of **1c** = 350 mg L^{-1} and 4-nitrophenol = 3.5×10^{-4} mol L^{-1} in DCM.

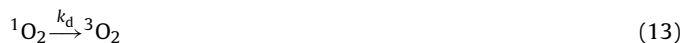The singlet oxygen quantum yields Φ_Δ were calculated using Eq. (12) [21].

$$\frac{1}{\Phi_{DPBF}} = \frac{1}{\Phi_\Delta} + \frac{1}{\Phi_\Delta} \cdot \frac{k_d}{k_a} \cdot \frac{1}{[DPBF]} \qquad (12)$$

where k_d is the decay constant of singlet oxygen in respective solvent and k_a is the rate constant of the reaction of DPBF with $O_2(^1\Delta_g)$. The intercept obtained from the plot of $1/\Phi_{DPBF}$ vs $1/DPBF$ gives $1/\Phi_\Delta$.

2.4. Kinetics of photosensitization

The quantum yields of phototransformation of 4-nitrophenol ($\Phi_{4\text{-NP}}$) were calculated using Eq. (10) and replacing DPBF with 4-NP. The determined molar exctinction coefficient of 4-NP (1.5×10^3 L mol^{-1} cm^{-1} at 400 nm) in DCM was used to calculate the concentration of 4-NP.

Assuming transformation of 4-NP follows Type II reaction pathway, rate constants involved are for the decay of $^1O_2$ (k_d, Eq. (13)), physical quenching of $^1O_2$ by the substrate (k_q, Eq. (14)) and the formation of oxidation products (k_r, Eq. (15)).

$$^1O_2 \xrightarrow{k_d} {}^3O_2 \qquad (13)$$

$$4\text{-NP} + {}^1O_2 \xrightarrow{k_q} {}^3O_2 \qquad (14)$$

$$4\text{-NP} + {}^1O_2 \xrightarrow{k_r} \text{products} \qquad (15)$$

Using Eqs. (13)–(15), the rate constants for the phototransformation of 4-NP may be calculated using Eq. (16) [21].

$$\frac{1}{\Phi_{4\text{-NP}}} = \frac{1}{\Phi_\Delta} \left(\frac{k_q + k_r}{k_r} + \frac{k_d}{k_r[4\text{-NP}]} \right) \qquad (16)$$

where Φ_Δ and $\Phi_{4\text{-NP}}$ are the singlet oxygen and 4-NP quantum yields. k_d is calculated using Eq. (16)

$$k_d = \frac{1}{\tau_\Delta} \qquad (17)$$

where τ_Δ is the lifetime of singlet oxygen in the solvent. k_d in DCM is 1.6×10^4 s^{-1} [22]. The rate constants k_q and k_r can be determined by plotting $1/\Phi_{4\text{-NP}}$ vs $1/[4\text{-NP}]$ using Eq. (17).

3. Results and discussions

3.1. Singlet oxygen quantum yields (Φ_Δ)

The energy transfer from an excited MPc to triplet oxygen affords singlet oxygen. Singlet oxygen plays an important role in oxidation reactions. Singlet oxygen quantum yield (Φ_Δ) values (Table 1) were determined using DPBF as the singlet oxygen quencher in DCM for photosensitized reaction. Based on the heavy atom effect, it would be expected that the PtPc complexes would give larger Φ_Δ values. However, the Φ_Δ value is slightly higher for PdPc **1e** compared to the corresponding PtPc complex **2e**. Complexes **1d** and **2d** show almost similar Φ_Δ values. The Φ_Δ values of both PtPc and PdPc complexes are however still sufficient for photosensitized transformation of 4-NP.

3.2. Effect of photosensitizer and 4-NP concentrations on phototransformation of 4-NP

These studies were carried out in DCM (basic media using triethylamine as an organic buffer) since the phenolate ions, which are more oxidizable, are predominant in basic media (pKa 4-NP = 7.15) [23]. Fig. 2 shows the spectral changes observed during homogeneous photolysis of 4-NP in the presence of complex **1c** (as an example). There is a decrease in the absorbance (at 400 nm) of 4-NP during irradiation (with time) in the presence of complex **1c**. The absorbance of complex **1c** was unchanged during the photolysis due to its high photostability as shown by the lack of change in the intensity of the Q-band of the MPc at 690 nm. The peak due to the phenolate ions at 400 nm started disappearing with simultaneous increase in the intensity of the peak at 260 nm due to the formation of the products. It has been reported before that the peak near 300 nm is due to conversion of the phenolate ions to the protonated form [23]. However since we are working in basic media, the protonation reaction is not expected. The B band of phthalocyanines occurs in the 300 nm region hence complicating the spectra. Thus the disappearance of 4-NP rather than formation of products was employed for the studies in this work. The $\Phi_{4\text{-NP}}$ were calculated from the initial rate of disappearance of the 4-NP using Eq. (10) (where DPBF is replaced by 4-NP).

Aggregation in MPc affects their photosensitization behavior. This is judged by a broadened and split Q band, with the blue shifted component being due to the aggregate. All the complexes were aggregated in DCM (Fig. 3) but were not aggregated in 1-chloronaphthalene (which was employed before for photophysical studies [18]). However DCM was found to be an appropriate solvent for this work. Fig. 3 shows that the most aggregated complex was **2e**, as judged by the enhanced absorption band due to aggregates near 600 nm, considering the same concentration of ∼1.0×10^{-5} M. This absorption band is more intense than the band due to the monomer near 660 nm for **2e**, showing extensive aggregation for this complex. Complex **1e** also showed an intense band due to the aggregate (Fig. 3), but aggregation was not as severe as for **2e**. The presence of aromatic substituents (in substituent **e**) lying in the same plane as the phthalocyanine ring is expected to promote aggregation due to strong π–π interaction. This explains why both **1e** and **2e** (both containing a more aromatic substituent) show more extensive aggregation than the rest of the complexes. Due to more extensive aggregation complex **2e** (in particular) is expected to give a low value for $\Phi_{4\text{-NP}}$. However, Table 1 shows that the largest $\Phi_{4\text{-NP}}$ values were obtained for complexes **1a–1c** and **1e**. Complexes **2e** and **2d** gave the lowest $\Phi_{4\text{-NP}}$ values. Low Φ_Δ values for Pt complexes would also give low $\Phi_{4\text{-NP}}$. Φ_Δ are also reduced by aggregated species which was more severe for **2e**.

The $\Phi_{4\text{-NP}}$ values obtained in the work are similar to those reported in aqueous media for the phototransformation of 4-NP using zinc tetrasulfo phthalocyanines (ZnPcS$_4$), zinc octacarboxyphthalocyanines (ZnPc(COOH)$_8$) and a sulfonated ZnPc sample containing a mixture of differently substituted sulfonated derivatives (ZnPcS$_{mix}$) [10]. ZnPc(COOH)$_8$ showed the best catalytic behavior [10], but degraded in solution, while the MPc complexes employed in this work do not show degradation.

The concentration of the catalyst will have an effect on phototransformation of the analyte. It is expected that the higher the
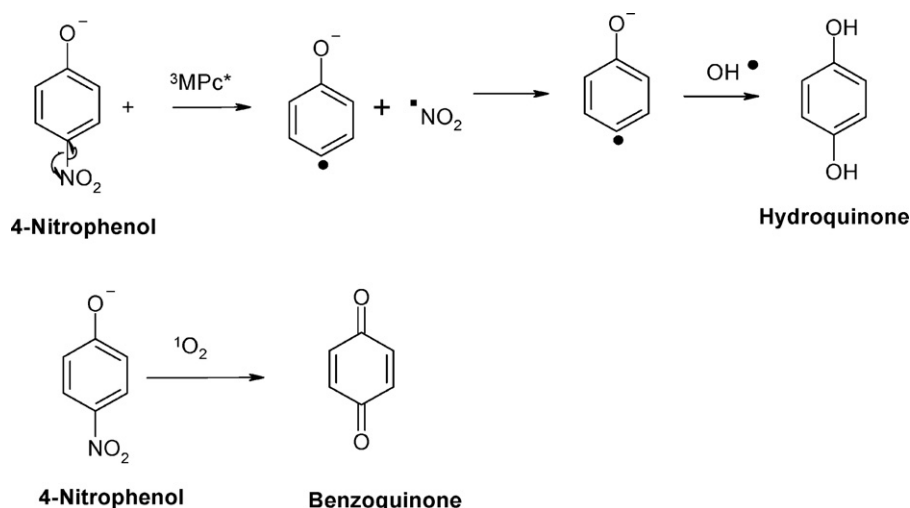
Scheme 1. Mechanism for oxidation of 4-nitrophenol.

catalyst concentration the higher the phototransformation of 4-NP. However as the concentration of the photosensitizers increases, aggregation increases (which reduces catalytic activity of the photosensitizers). Experiments were conducted where $\Phi_{4\text{-NP}}$ values were calculated at different concentrations of the photosensitizers ranging from $50\,\text{mg}\,\text{L}^{-1}$ to $500\,\text{mg}\,\text{L}^{-1}$ (Fig. 4) (using **1c** as an example and $[4\text{-NP}] = 3.5 \times 10^{-4}\,\text{mol}\,\text{L}^{-1}$). As the concentration of the MPc increased, the $\Phi_{4\text{-NP}}$ values increased until a maximum was reached and then there was a slight decline (Fig. 4). The decrease in $\Phi_{4\text{-NP}}$ with increase in photosensitizer concentration could be due to extensive aggregation of the molecules at high concentrations. The optimum concentrations of the photosensitizers were $200\,\text{mg}\,\text{L}^{-1}$ for **1a** and **2d**, $250\,\text{mg}\,\text{L}^{-1}$ for **1d**, $300\,\text{mg}\,\text{L}^{-1}$ for **1b**, $350\,\text{mg}\,\text{L}^{-1}$ for **1c**, **1e** and **2e** at 4-NP concentration of $3.5 \times 10^{-5}\,\text{mol}\,\text{L}^{-1}$ (Table 1). A linearity of $\Phi_{4\text{-NP}}$ vs 4-NP concentration (Fig. 5), was observed for concentrations less than $3.5 \times 10^{-5}\,\text{mol}\,\text{L}^{-1}$, hence below this concentration, $\Phi_{4\text{-NP}}$ may be accurately determined.

3.3. Kinetics of photosensitized reactions

The rate constant for photo-oxidation, k_r, was estimated from the slope of the plot of $1/\Phi_{4\text{-NP}}$ vs $1/[4\text{-NP}]$ (Fig. 6, using **1a**, **1c** and **1e** as examples). k_r equals k_d/Φ_Δ slope where k_d is the singlet oxygen decay constant in DCM ($1.6 \times 10^4\,\text{s}^{-1}$ [22]), and Φ_Δ is the singlet oxygen quantum yield of the sensitizer in DCM.

Using k_r values as an indication of phototransformation efficiency, Table 1 shows that photosensitized oxidation of 4-NP occurred faster when complexes **2d** and **2e** were used as sensitizers, with complex **1d** showing the lowest rate towards the photooxidation of 4-NP. The values k_r reported in this work for homogeneous phototransformation of 4-NP are much lower that the values obtained for sulfonated AlPc derivatives (order of $10^8\,\text{mol}^{-1}\,\text{L}\,\text{s}^{-1}$) [24] for the oxidation of chlorophenols.

The quenching effect of the 4-NP on the singlet oxygen was estimated from $(k_q + k_r)$ calculated from the intercept of the plot of $1/\Phi_{4\text{-NP}}$ vs $1/[4\text{-NP}]$. Comparison of the $(k_q + k_r)$ with k_r or estimation of k_q from the two gives the deactivation or quenching of singlet oxygen via other routes apart from oxidation reaction with 4-nitrophenol. The values of $(k_q + k_r)$ for the sensitizers employed in this work ranged between 3.2×10^7 and $1.6 \times 10^9\,\text{mol}^{-1}\,\text{dm}^3\,\text{s}^{-1}$ while k_r ranged between 1.4×10^5 and $2.3 \times 10^5\,\text{mol}^{-1}\,\text{dm}^3\,\text{s}^{-1}$ (Table 1). The implication of large $(k_q + k_r)$ compared to k_r for all the sensitizers is that considerable amount of physical quenching of singlet oxygen took place during the reactions for all the com-

plexes. The $(k_q + k_r)$ values arrived at in this work are comparable with value of $2.8 \times 10^8\,\text{mol}^{-1}\,\text{dm}^3\,\text{s}^{-1}$ obtained previously [10].

3.4. Photosensitized transformation products and mechanism

GC and LC–MS were used to determine the products of phototransformation process by comparing the retention times of possible standards such as fumaric acid, 4-nitrocatechol, 1,4-benzoquinone and hydroquinone which are expected for the phototransformation of 4-nitrophenol. From comparison with the retention times of the standards, two new peaks (hydroquinone at retention time of 5.4 min and 1,4-benzoquinone at retention time 2.9 min) were observed in the gas chromatogram traces (Fig. 7), after irradiation for 12 h. The peak due to 4-NP (retention time = 2.3 min) was decreased in intensity. These peaks were all confirmed using GC analysis by spiking with the respective standards. The LC–MS chromatograms also showed peaks corresponding to residual 4-nitrophenol (retention time = 15 min), hydroquinone (retention time = 5.5 min) and benzoquinone at a retention time of 9 min. The results from direct injection into mass spectrometer showed the formation of benzoquinone and hydroquinone with masses of 108.7 amu and 109.6 amu representing the molecular ions of benzoquinone and hydroquinone respectively. This, together the GC and HPLC–UV detection analyses allows us to be confident about the products formed. According to the chromatograms, hydroquinone was the major product while benzoquinone, which was expected to be the final product, was present in small quantity.

The mechanism for the phototransformation process was determined by using complex **1c** in the presence of sodium azide which is a singlet oxygen scavenger. While the rate of reaction was much faster in the absence of NaN$_3$ (presence of singlet oxygen), there was still 4-NP transformation happening in its presence (absence of singlet oxygen) (Fig. 8), meaning that the reaction proceeded through both Type I and Type II mechanisms. The rate of the reaction when the reaction medium was deareated by bubbling argon for 30 min was similar to what was obtained in the presence of sodium azide and the only product noticed here was hyroquinone. The implication was that the two products might be produced through different path ways. Hydroquinone through Type I and benzoquinone through Type II reactions, see Scheme 1. Based on this result the proposed mechanism is shown in Scheme 1. The triplet state molecules interact with deprotonated 4-nitrophenol (through Type I mechanism, Eq. (3)) to generate a phenolate radical. The protons interacted with OH$^-$ supplied by the basic media

to give water which on reaction with triplet state molecules generated OH$^\bullet$ radical which in turn reacted with phenolate radicals to produce hydroquinone. The production of benzoquinone was likely from the direct oxidation of 4-Np by singlet oxygen as reported in the photo-oxidation of 4-chlorophenol [25] (Scheme 1).

4. Conclusions

This work demonstrates that the complexes investigated are capable of photo-oxidation of 4-nitrophenol and PdPcs are better photosensitizers than PtPcs, with palladium octakis(dodecylthio)phthalocyanine (**1c**) giving the best performance in terms of the highest 4-NP phototransformation quantum yield. All the complexes showed no degradation during photolysis, and hydroquinone and benzoquinone were observed as the phototransformation products.

Acknowledgements

References

[1] A.P. Castanoa, T.N. Demidovaa, M.R. Hamblin, Photodiag. Photodyn. Ther. 1 (2004) 279.

[2] R. Bonnett, Chemical Aspect of Photodynamic Therapy, Gordon and Breach, London, 2000, pp. 70–74.

[3] R. Gerdes, D. Wohrle, W. Spiller, G. Schneider, G. Schulz-Ekloff, J. Photochem. Photobiol. A: Chem. 111 (1997) 65.

[4] T.C. Oldham, D. Phillips, J. Photochem. Photobiol. B: Biol. 55 (2000) 16.

[5] M.C. DeRossa, R.J. Crutchley, Coord. Chem. Rev. 233–234 (2002) 351.

[6] X.-F. Zang, H.-J. Xu, J. Chem. Soc. Faraday Trans. 89 (1993) 3347.

[7] A. Ogunsipe, J.-Y. Chen, T. Nyokong, New J. Chem. 28 (2004) 822.

[8] H. Ali, J.E. Van Lier, Chem. Rev. 99 (1999) 2379.

[9] D.M. Guldi, T.D. Mody, N.N. Gerasimchuk, D. Magda, J.L. Sessier, J. Am. Chem. Soc. 122 (2000) 8289.

[10] E. Marais, R. Klein, E. Antunes, T. Nyokong, J. Mol. Catal. A: Chem. 261 (2007) 36.

[11] A.E.H. Machado, J.A. de Miranda, R.F. de Freitas, E.T.F.M. Duarte, L.F. Ferreira, Y.D.T. Albuquerque, R. Ruggiero, C. Sattler, L.J. de Oliveira, Photochem. Photobiol. A: Chem. 155 (2003) 231.

[12] V.J. Iliev, Photochem. Photobiol. A: Chem. 151 (2002) 195.

[13] R. Gerdes, D. Wöhrle, W. Spiller, G. Schneider, G. Schnurpfeil, G.J. Schulz-Ekloff, Photochem. Photobiol. A: Chem. 111 (1997) 65.

[14] Z. Xiong, Y. Xu, L. Zhu, J. Zhao, Environ. Sci. Technol. 39 (2005) 651.

[15] Q. Sun, Y. Xu, J. Phys. Chem. C 113 (2009) 12387.

[16] Y. Xu, Z. Chen, Chem. Lett. 32 (2003) 592.

[17] P. Kluson, M. Drobek, S. Krejcikova, J. Krysa, A. Kalaji, T. Cajthaml, J. Rakusan, Appl. Catal. B: Environ. 80 (2008) 321.

[18] T.B. Ogunbayo, T. Nyokong, J. Mol. Struct. 973 (2010) 96.

[19] A. Sun, Z. Xiong, Y. Xu, J. Hazard. Mater. 152 (2008) 191.

[20] X. Xue, Y. Xu, J. Mol. Catal. 276 (2007) 80.

[21] W. Spiller, H. Kliesch, D. Worhle, S. Hackbarth, B. Roder, G. Schnurpfield, J. Porphyrins Phthalocyanines 2 (1998) 145.

[22] F. Wilkinson, J.G. Brummer, J. Phys. Chem. Ref. Data 10 (1981) 825.

[23] A.P. Terzyk, M. Wśniewski, P. Gauden, G. Rychlicki, S. Furmaniak, J. Colloid Interface Sci. 320 (2008) 40.

[24] K. Ozoemena, N. Kuznetsova, T. Nyokong, J. Mol. Catal. A: Chem. 176 (2001) 29.

[25] E. Sibva, M.M. Pereira, H.D. Burrows, M.E. Azenha, M. Sarakha, M. Bolte, Photochem. Photobiol. Sci. 3 (2004) 200.